JOURNAL OF GEOPHYSICAL RESEARCH, VOL. 103, NO. A9, PAGES 20,643–20,649, SEPTEMBER 1, 1998

A model for pickup ion transport in the heliosphere in the limit of uniform hemispheric distributions

N. A. Schwadron

Department of Atmospheric, Oceanic and Space Sciences, University of Michigan, Ann Arbor

Abstract. On the basis of recent observations that pickup ions are inefficiently scattered through 90° pitch angle, a pickup ion transport model has been developed which assumes that pickup ion distributions are uniform in the so-called forward and reverse hemispheres, containing ions with pitch angles less than 90° and greater than 90°, respectively. A simple, fast numerical scheme is then described which solves the transport equations. Several examples are solved and comparisons are performed between the numerical solutions and previously used analytical solutions. Results from the model are then compared to pickup ion spectra obtained with the solar wind ion composition spectrometer on the Ulysses satellite.

1. Introduction

Pickup ions in a magnetized plasma are produced when neutral particles from, for example, comets, the interstellar gas, or interplanetary dust, are ionized due to photoionization, charge exchange, or electron impact ionization. The result is an ion which is suddenly injected into the magnetized plasma and instantaneously experiences the Lorentz force exerted by the plasma's magnetic field. In the frame of reference moving with the plasma, the ion will begin to gyrate about the plasma's magnetic field and stream along the magnetic field lines. The pickup particles are then subject to ion scattering and acceleration as they encounter magnetic irregularities embedded in the plasma.

Considerable attention has been recently focused on the dynamical properties of interstellar pickup hydrogen and helium [*Gloeckler et al.*, 1995; *Fisk et al.*, 1997; *Möbius et al.*, 1998]. One of the main surprises, reported initially by *Gloeckler et al.* [1995], was that at high latitudes, pickup hydrogen has a sizable anisotropy, consistent with a scattering mean free path of $\lambda \sim 2$ astronomical units (AU, hereafter). Quasi-linear models of wave-particle interactions and their many non linear extensions predict much smaller mean free paths for ions of such low rigidity [e.g., *Palmer*, 1982; *Bieber et al.*, 1994], assuming that the magnetohydrodynamic turbulence is composed of principally slab type, or one-dimensional, fluctuations. Recently, however, it has been demonstrated that quasi-linear models which incorporate a composite of slab and two-dimensional fluctuations predict much larger parallel mean free paths [*Bieber et al.*, 1994; *Zank et al.*, 1998]; this is consistent with observations of a dominant two-dimensional component of field fluctuations in the inertial range [*Matthaeus et al.*, 1990; *Bieber et al.*, 1996].

Evidence was provided by *Fisk et al.* [1997] that the cause of the long mean free path was a low scattering rate through 90° pitch angle (the pitch angle is the angle between the ion velocity in the solar wind reference frame and the magnetic field direction). This evidence suggests, in fact, that pickup particles may be uniform in the forward and reverse hemispheres, with pitch angles $\theta < 90°$ and $\theta > 90°$, respectively (i.e., the distributions are apparently isohemispheric). Of course, the large anisotropy implies that there a far more ions in the reverse than forward hemispheres.

An analytic model for pickup ion transport in the limit that scattering is strongly inhibited only at 90° pitch angle was provided by *Isenberg* [1997]. The model assumed that the scattering rate scaled as v/r (where v is the ion speed in the solar wind rest frame and r is the radial distance from the Sun) and that the magnetic field was entirely radial. An attempt to fit the detailed spectrum of *Isenberg* [1997] to a spectrum observed with the solar wind ion composition spectrometer on Ulysses was not successful.

The purpose of this paper is to provide a numerical tool which may be used to fit pickup ion spectra in the solar wind over a wide range of conditions. We will provide general equations for pickup ion transport under the assumption that the particle distributions are uniform in the forward and reverse hemispheres. The treatment in this paper neglects statistical and shock acceleration. We will provide a fast, simple, and versatile numerical technique for solving the transport equations and illustrate solutions for several simple cases. Comparisons are performed between the numerical solutions and previously used analytical solutions. Results from the model are then compared to pickup ion spectra obtained with the Solar Wind Ion Composition Spectrometer on the Ulysses satellite.

Paper number 98JA01686.
0148-0227/98/98JA-01686$09.00

2. Pickup Ion Transport Equations for Uniform Hemispheric Distributions

In this section, we will derive the transport equations for pickup ions assuming that the pickup ions distribution is uniform in the forward and reverse hemispheres:

$$f(\mathbf{r}, v, \mu) = f_+(\mathbf{r}, v)\Theta(\mu) + f_-(\mathbf{r}, v)\Theta(-\mu) \quad (1)$$

where f_+ (f_-) is the uniform distribution of ions in the forward (reverse) hemisphere, v is the pickup speed in the solar wind reference frame, $\mathbf{r}$ is the heliospheric position, and μ is the pitch angle cosine. The step function $\Theta(x)$ is defined such that $\Theta(x) = 1$ for $x > 0$ and $\Theta(x) = 0$ for $x < 0$.

The full transport equation for pickup ions assumes that the pickup ions are gyrotropic and that the plasma flows with constant speed: $\partial \mathbf{u}/\partial t = 0$ and $\nabla u^2 = 2(\mathbf{u} \cdot \nabla)\mathbf{u} = 0$, where $\mathbf{u}$ is the plasma bulk velocity. The transport equation includes the effects of convection, adiabatic focusing, adiabatic cooling, and pitch angle scattering. It is written here in the spatial reference frame of an inertial observer such as a spacecraft or the Sun and the velocity reference frame of the plasma [*Skilling*, 1971]

$$\begin{aligned}\frac{\partial f}{\partial t} + (\mathbf{u} + \mathbf{v}_\parallel) \cdot \nabla f + \nabla \cdot (v\hat{\mathbf{e}}_B)\frac{1-\mu^2}{2}\frac{\partial f}{\partial \mu} - \\ \nabla \cdot \mathbf{u}\frac{1-\mu^2}{2}v\frac{\partial f}{\partial v} + \nabla \cdot \mathbf{u}\frac{1-\mu^2}{2}\mu\frac{\partial f}{\partial \mu} + \\ \hat{\mathbf{e}}_B \cdot [(\hat{\mathbf{e}}_B \cdot \nabla)\mathbf{u}]\left(\frac{1-3\mu^2}{2}v\frac{\partial f}{\partial v} - \right. \\ \left. 3\frac{1-\mu^2}{2}\mu\frac{\partial f}{\partial \mu}\right) = \left(\frac{\delta f}{\delta t}\right)_{scatt} + Q(\mathbf{r}, v, \mu) \quad (2)\end{aligned}$$

where the pickup ion distribution function averaged over a gyroperiod is given by $f(t, \mathbf{r}, v, \mu)$; $\mathbf{v}_\parallel = v\mu\hat{\mathbf{e}}_B$ is the pickup ion velocity parallel to the magnetic field; and $\hat{\mathbf{e}}_B$ is a unit vector in the direction of the magnetic field. $Q(\mathbf{r}, v, \mu)$ is the pickup ion source term, and $(\delta f/\delta t)_{scatt}$ is the scattering term, each of which will be discussed below.

The pickup ion source term may be generally written as follows:

$$Q(v, \mu, r) = \beta_p(\mathbf{r})n_n(\mathbf{r})\frac{\delta(v-u)}{2\pi u^2}S(\mathbf{r}, \mu). \quad (3)$$

Here $n_n(\mathbf{r})$ is the neutral density at the heliospheric position, $\mathbf{r}$; $S(\mathbf{r}, \mu)$ represents the initial pitch angle distribution normalized such that $\int_{-1}^{1} d\mu\, S(\mu) = 1$; and $\beta_p(\mathbf{r})$ is the production rate. In many applications, the production rate is assumed to fall off as $\beta_p(\mathbf{r}) = \beta_p(r_1)(r_1/r)^2$ (r_1 represents 1 AU and $\beta_p(r_1)$ is the production rate referenced to r_1), since photoionization and charge exchange scale with the photon density and proton density which fall off as $1/r^2$.

For the scattering term on the right-hand side of (2), we assume that ions are scattered efficiently in the forward and reverse hemispheres but have difficulty scattering through 90° pitch angle:

$$\begin{aligned}\left(\frac{\delta f}{\delta t}\right)_{scatt} = & -\frac{f - f_+}{\tau'}\Theta(\mu) - \frac{f_+ - f_-}{\tau}\Theta(\mu) - \\ & \frac{f - f_-}{\tau'}\Theta(-\mu) - \frac{f_- - f_+}{\tau}\Theta(-\mu) \quad (4)\end{aligned}$$

Here the rate of scattering through 90° pitch angle is given by $1/\tau$, and the rate of scattering within each hemisphere is given by $1/\tau'$. The assumption that the distributions are uniform in each hemisphere is equivalent to the assumption that the scattering rate in each hemisphere, $1/\tau'$, is larger than all other physical rates in the problem: $1/\tau' \gg 1/\tau$, $|(1/f)\mathbf{v}_\parallel \cdot \nabla f|$, $|(1/f)v\partial f/\partial v|$, $|(1/f)\nabla \cdot \mathbf{u}\partial f/\partial \mu|$, β_p, etc.. In this case, $f = f_+\Theta(\mu) + f_-\Theta(-\mu)$ is the lowest order eigenfunction of the ratewise dominant operator $-(f - f_+)/\tau' - (f - f_-)/\tau'$ with eigenvalue 0. Hence (1) represents the lowest order pitch angle distribution consistent with the scattering operator (4).

The relaxation approximation (4) described here is often replaced by a Fokker-Planck pitch angle diffusion term:

$$\left(\frac{\delta f}{\delta t}\right)_{scatt} = \frac{\partial}{\partial \mu}\left[\Phi(\mu)(1-\mu^2)\frac{\partial f}{\partial \mu}\right] \quad (5)$$

This form of the scattering term results from quasilinear models of wave-particle interaction in which inhibited scattering through 90° pitch angle naturally results from a resonance gap in the interaction between ions and parallel propagating waves [e.g., *Rowlands et al.*, 1966; *Dusenbery and Hollweg*, 1981]. The treatment of the resonance gap and potentially nonlinear processes which would determine its character is beyond the scope of this paper. However, if it is assumed that the distribution is uniform in each hemisphere (1), the relaxation-time approximation for scattering through 90° pitch angle may be related directly to the Fokker-Planck operator:

$$\frac{f_+ - f_-}{\tau} = \Phi(0)\frac{\partial f(\mu = 0)}{\partial \mu} \quad (6)$$

or, equivalently, $1/\tau = \Phi(0)/\delta$, where δ is a measure of the pitch angle width of the transition between f_- and f_+ near 90° pitch angle.

Multiplying (2) by the operators $[\Theta(\mu) \pm \Theta(-\mu)]/2$ and integrating over μ yields the following transport equations:

$$\frac{Df_0}{Dt} + \nabla \cdot (v\hat{\mathbf{e}}_B\Delta/2) - (\nabla \cdot \mathbf{u}/3)v\frac{\partial f_0}{\partial v} = 1/2\int_{-1}^{1} d\mu Q(v, \mu, \mathbf{r}) \quad (7)$$

$$\frac{D\Delta}{Dt} + v\hat{\mathbf{e}}_B/2 \cdot \nabla f_0 - (\nabla \cdot \mathbf{u}/3)v\frac{\partial \Delta}{\partial v} = -2\Delta/\tau + 1/2\int_{-1}^{1} d\mu[\Theta(\mu) - \Theta(-\mu)]Q(v, \mu, \mathbf{r}) \quad (8)$$

Here $f_0 = (f_+ + f_-)/2$ is the isotropic part of the distribution function and $\Delta = (f_+ - f_-)/2$ is the anisotropic part of the distribution function. The convective derivative is defined $D/Dt \equiv \partial/\partial t + \mathbf{u}\cdot\nabla$.

3. A Numerical Algorithm for Obtaining Solutions

In this section we will develop a numerical algorithm for solving the pickup ion transport equations, assuming steady state, and that the the plasma undergoes a radial expansion, $\nabla\cdot\mathbf{u} = 2u/r$. The numerical scheme may be generalized to cases of nonradial expansions (N. A. Schwadron et al., Pronounced enhancements of pickup hydrogen and helium in high-latitude compressional regions, submitted to *Journal of Geophysical Research*, 1998, hereinafter referred to as submitted manuscript).

The steady state pickup ion transport equations may be transformed into a much simpler form by using the dimensionless coordinates $w = v/u$ and $y = (r/r_1)w^{3/2}$, where r_1 denotes 1 AU, and dimensionless functions $\tilde{f}_0 = u^3 f_0/n_0$ and $\tilde{\Delta} = u^3\Delta/n_0$, where n_0 is a reference density:

$$\frac{\partial \tilde{f}_0}{\partial w} = 3\xi(\mathbf{r})\tilde{\Delta}/4 + \frac{3\alpha(\mathbf{r})y}{4}\frac{\partial\tilde{\Delta}}{\partial y} \tag{9}$$

$$\frac{\partial}{\partial w}\left[\exp(2yw^{-3/2}r_1/\lambda)\tilde{\Delta}\right] = \exp(2yw^{-3/2}r_1/\lambda)\cdot \left(\frac{3\alpha(\mathbf{r})y}{4}\frac{\partial\tilde{f}_0}{\partial y}\right) \tag{10}$$

where we take the boundary conditions,

$$\tilde{f}_0(v/u\sim 1,\mathbf{r}) = \frac{3}{8\pi}\frac{r\beta_p(\mathbf{r})}{u}\frac{n_n(\mathbf{r})}{n_0} \tag{11}$$

$$\tilde{\Delta}(v/u\sim 1,\mathbf{r}) = \frac{3}{8\pi}\frac{r\beta_p(\mathbf{r})}{u}\frac{n_n(\mathbf{r})}{n_0}\cdot \int_{-1}^{1} d\mu[\Theta(\mu)-\Theta(-\mu)]S(\mathbf{r},\mu) \tag{12}$$

Here the dimensionless quantities $\xi(\mathbf{r})$, and $\alpha(\mathbf{r})$ are given by $\xi = r\nabla\cdot\hat{\mathbf{e}}_B$ and $\alpha = \hat{\mathbf{e}}_B\cdot\hat{\mathbf{e}}_r \equiv \cos(\psi)$, where $\hat{\mathbf{e}}_r$ is the unit vector in the radial direction and ψ is the angle between the magnetic field and the radial direction.

The numerical algorithm is obtained by discretizing $\tilde{f}_0(y,w)$, $\tilde{\Delta}(y,w)$, $\alpha(y,w)$, and $\xi(y,w)$ for $y_i = r_0/r_1 + (i-1)\Delta y$ and $w_j = (j-1)\Delta w$ with $i = 1\ldots M$, $j = 1\ldots N$, $y_M = r/r_1$, and $w_N = 1$. Using second-order central differencing for the differential operators in (9) and (10), we obtain a set of explicit iterative equations for $\tilde{f}_{0i}^{\,j}$ and $\tilde{\Delta}_i^j$:

$$\tilde{f}_{0i}^{\,j-1} = \tilde{f}_{0i}^{\,j+1} - \frac{3\Delta w}{4\Delta y}\alpha_i^j y_i(\tilde{\Delta}_{i+1}^j - \tilde{\Delta}_{i-1}^j) - \frac{3\Delta w}{2}\xi_i^j\tilde{\Delta}_i^j$$

$$\tilde{\Delta}_i^{j-1} = \exp\left[-\frac{2r_1y_i}{\lambda}(w_{j-1}^{-3/2} - w_{j+1}^{-3/2})\right]\tilde{\Delta}_i^{j+1} \tag{13}$$

$$-\exp\left[-\frac{2r_1y_i}{\lambda}(w_{j-1}^{-3/2} - w_j^{-3/2})\right]\cdot \frac{3\Delta w}{4\Delta y}\alpha_i^j y_i(\tilde{f}_{0i+1}^{\,j} - \tilde{f}_{0i-1}^{\,j}) \tag{14}$$

A requirement for stability is that $\Delta w < \Delta y$.

The procedure is straightforward: we set the boundary conditions at w_N and w_{N-1}; starting at $j = N-1$, the upper boundary of the dimensionless velocity grid $w_{N-1} = 1-\Delta w$, we obtain solutions for $\tilde{f}_{0i}^{\,N-2}$ and $\tilde{\Delta}_i^{N-2}$ by iterating equations (13) from $i = 1$ to $i = M$. We iteratively repeat this procedure from $j = N-3$ down to $j = 1$. Once a solution is obtained on the grid for the coordinates y and w, it must be mapped to the standard coordinates, r and v. The scheme is explicit and quite fast. A typical integration time on a workstation is 30 seconds.

4. Several Simple Examples

In this section, we will consider several examples of solutions. In the first example, we will consider an interstellar hydrogen source and in the second example, a localized source at $r < r_1$ will be considered.

In each of the examples, we will assume that magnetic field assumes a standard Archimedes spiral pattern [*Parker*, 1958]. Hence

$$\begin{aligned}\alpha(r) &= [1+(\Omega r\sin\theta_{\rm H}/u)^2)]^{-1/2}\\ \xi(r) &= [2+(\Omega r\sin\theta_{\rm H}/u)^2)]\alpha(r)^3\end{aligned} \tag{15}$$

where Ω is the Sun's rotation rate and $\theta_{\rm H}$ is the polar angle of the spacecraft measured from the Sun's rotation axis.

The source term in these examples assumes that ions are picked up in the reverse hemisphere, and that the production rate scales as $1/r^2$:

$$Q(v,\mu,r) = \beta_p(r_1/r)^2 n_n(r)\frac{\delta(v-u)}{2\pi u^2}\Theta(-\mu) \tag{16}$$

Two limits of the mean free path will be considered: $\lambda = 1$ AU and $\lambda = 0.01$ AU. In the case of a short mean free path, the anisotropy Δ must become small, and $f_0(r,w)$ must converge on the analytic solution with $\lambda\to 0$ [*Vasyliunas and Siscoe*, 1976]:

$$f_0(r,w) \overset{\lambda\to 0}{=} \frac{3\beta_p r_1^2}{8\pi u^4 r w^{3/2}} n_n(rw^{3/2}) \tag{17}$$

for $v \le u$, and for $v > u$, $f_0 = 0$. This poses a stringent test for the numerical solution.

It is also possible to obtain an analytic solution for the distribution function in the limit that the anisotropies are small: $\Delta/f_0 \ll 1$. In this case, the anisotropy is purely diffusive and according to (8), we may write the anisotropy as $\Delta = -(v\tau/4)\hat{\mathbf{e}}_B\cdot\nabla f_0$. A diffusion equation for f_0 is obtained when this approximation for the anisotropy is used in (7). An analytic solution for f_0

may then be obtained by making the following assumptions: (1) steady state; (2) that the solar wind undergoes a radial expansion; and (3) that the effective mean free path $\lambda' = \tau v \cos^2(\psi)$ is constant:

$$\begin{aligned} f_0(r,v) &= \frac{5r_1}{\pi u^4}\frac{r_1}{\lambda'}\frac{\beta_p}{z^{1/2}w^{3/4}}\frac{1}{1-w^{5/2}}\int_0^\infty \frac{dz'}{z'^{1/2}} \\ &\cdot\ n_n(z')\exp\left(-\frac{40r_1}{3\lambda'}\frac{zw^{3/2}+z'}{1-w^{5/2}}\right) \\ &\cdot\ I_1\left(\frac{80r_1}{3\lambda'}\frac{(z'z)^{1/2}w^{3/4}}{1-w^{5/2}}\right) \end{aligned} \quad (18)$$

for $v \leq u$, and for $v > u$, $f_0 = 0$. Here we use the dimensionless coordinates $z = r/r_1$, $w = v/u$, and I_1 is a first-order modified Bessel function.

In the two simple examples discussed below, we will perform comparisons between the numerically calculated distributions, the fully isotropic distribution (17), and the solution in the purely diffusive limit (18).

4.1. Example 1: An Interstellar Hydrogen Source

An approximation for an interstellar neutral hydrogen density in the heliosphere is given by

$$n_H = n_\infty \exp(-4r_1/r). \quad (19)$$

Using this expression in the source term (16), we obtain solutions for f_+ and f_- at $r = 3.5$ AU and $\theta_H = 40°$. Plotted in Figure 1 are the solutions as a function of $w = v/u$. AU. In these calculations, we have taken $u = 800$ km/s, $n_\infty = 1$ cm^{-3}, and $\beta_p(r_1) = 2 \cdot 10^{-7}$.

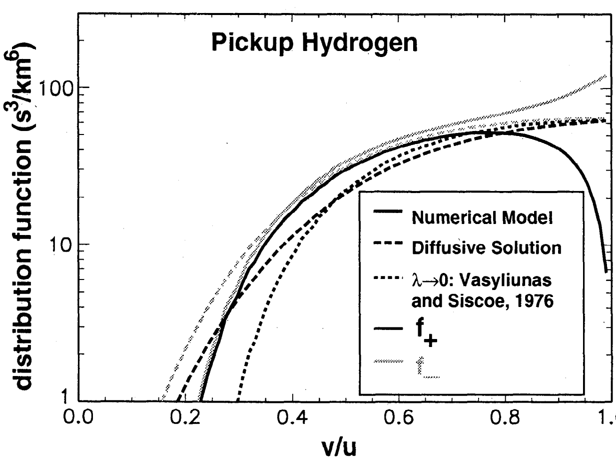

Figure 1. Comparisons between the numerical model (solid curves) for a 1 AU mean free path, the purely diffusive solution (long-dashed curves) expressed in (18) for a 1 AU mean free path, and the solution in the limit of a short mean free path (short-dashed curve) expressed in equation (17). In this case, the source of pickup ions is interstellar hydrogen. Black (grey) curves represent the distribution in the forward (reverse) hemisphere, f_+ (f_-). In the limit of a short mean free path, the forward and reverse hemisphere distributions become equal to the isotropic distribution: $f_+ = f_- = f_0$. The parameters and source function used in the calculations are described in section 4.1.

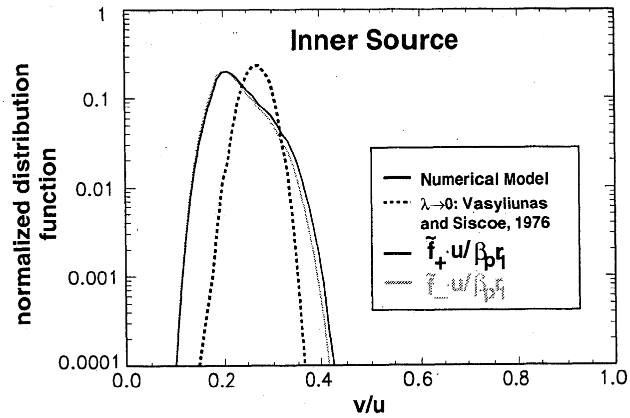

Figure 2. Comparisons between the numerical model (solid curves) for a 1 AU mean free path, and the solution in the limit of a short mean free path (dashed curve) expressed in equation (17) for a source of pickup ions localized close to the Sun. The black curve represents the normalized distribution in the forward hemisphere, $\tilde{f}_+ u/[r_1\beta_p(r_1)]$, and the grey curve represents the normalized distribution in the reverse hemisphere, $\tilde{f}_- u/[r_1\beta_p(r_1)]$. In the limit of a short mean free path the forward and reverse hemisphere distributions become equal to the isotropic distribution: $f_+ = f_- = f_0$. The parameters and source function used in the calculations are described in section 4.2.

Plotted as the solid black (grey) curve in Figure 1 is the numerical solution for f_+ (f_-) given a mean free path of $\lambda = 1$ AU. Plotted as the long-dashed black (grey) curve is the purely diffusive solution (18) for f_+ (f_-) given a mean free path of $\lambda = 1$ AU. Also plotted as the short-dashed black curve is the analytic solution for f_0 in the limit of a small mean free path (17). In the limit of a short mean free path, both the numerical solution and the purely diffusive solution reproduce the analytic solution for f_0 given by (17).

4.2. Example 2: An Inner Source

For the second example, we will consider a source of pickup ions which is localized close to the Sun. In this case, we take the source density:

$$n_n = n_0 \exp[-(r - r_0)^2/dr^2] \quad (20)$$

where $r_0 = 0.5$ AU and $dr = 0.1$ AU. Using this expression in the source term (16), we obtain solutions for $\tilde{f}_+ u/[r_1\beta_p(r_1)]$ and $\tilde{f}_- u/[r_1\beta_p(r_1)]$ at $r = 3.5$ AU and $\theta_H = 40°$. As in the first example, we take $u = 800$ km/s.

Plotted as the solid black curve in Figure 2 is the numerical solution for $\tilde{f}_+ u/[r_1\beta_p(r_1)]$ (the grey curve represents the solution for $\tilde{f}_- u/[r_1\beta_p(r_1)]$) given a mean free path of $\lambda = 1$ AU. Also plotted as the dashed black curve is the analytic solution for $\tilde{f}_0 u/[r_1\beta_p(r_1)]$ in the limit of a small mean free path (17). The purely diffusive solution (18) becomes unreasonable in this case due to the large gradients close to the Sun. Again, in the limit of a short mean free path, the numerical solution reproduces the analytic solution for f_0 given by (17).

5. Detailed Fits to Observed Spectra

In this section, we will consider detailed fits of the numerically computed pickup ion distributions to spectra obtained with the solar wind ion composition spectrometer (SWICS) on the Ulysses satellite. We will examine hydrogen and helium spectra observed between day 220 and 280 of 1994, while the Ulysses spacecraft was near 2.3 AU at a latitude of $-80°$.

The data presented here were obtained with the SWICS instrument [*Gloeckler et al.*, 1992] on Ulysses. SWICS measures the intensity of solar wind and suprathermal ions as a function of their energy per charge (E), mass (m), and charge state (q), from 0.6 to 60 keV/e in logarithmically spaced steps with $\Delta E/E \approx 0.04$. SWICS uses techniques of energy per charge analysis, followed by post acceleration of the ions by 23 kV and a time-of-flight and energy measurement, to identify ions and sample their distributions once every 13 min. With the double and triple coincidence techniques used, the background levels are extremely low allowing measurements of very low flux levels of interstellar pickup ions. The viewing angle of SWICS is such that in one spin period ($\sim$ 12 s) a π steradian cone, centered within 20° of the solar wind direction is sampled.

The observed distribution function of pickup ions, $f'(v')$, is measured in the frame of reference of the spacecraft and is therefore the distribution function in the solar wind reference frame $f(\mathbf{v})$, averaged over the acceptance angles of SWICS:

$$f'(v') = 1/\pi \int d\Omega' f(\mathbf{v} = v'\hat{\mathbf{e}}' - \mathbf{u}). \qquad (21)$$

Here v' is the ion speed in the spacecraft frame, $\mathbf{v}$ is the ion velocity in the solar wind frame, $\mathbf{u}$ is the solar wind velocity, $\hat{\mathbf{e}}'$, is a unit vector pointing in a direction at which the instrument accepts incoming ions, and the angular integral, $\int d\Omega'$, integrates $\hat{\mathbf{e}}'$ over all instrument acceptance angles. Note that SWICS is configured such that $\int d\Omega' = \pi$.

For the calculation of the pickup ion distributions, we will again assume that the magnetic field resembles the standard Archimedes spiral pattern. Therefore the variables $\alpha(r)$ and $\xi(r)$ are given by (15). For the source term, we assume that all ions are picked up in the reverse hemisphere ($\mu < 0$):

$$Q(v,\mu,r) = \beta_p(r_1)(r_1/r)^2 n_n(r)\frac{\delta(v-u)}{2\pi u^2}\Theta(-\mu). \qquad (22)$$

where $n_n(\mathbf{r})$ is the interstellar neutral density at the heliospheric position, $\mathbf{r}$.

For the interstellar neutral density, $n_n(r, \theta_{Int}; \beta_L, T, n_\infty, v_0, \mu_0)$, we use the "hot" model [*Fahr*, 1971; *Thomas*, 1978; *Wu and Judge*, 1979] which yields the density as a function of radial distance, the angle between the radial direction and the upwind direction of the interstellar neutrals, θ_{Int}. The neutral density in the hot model also depends implicitly on the temperature of the neutrals, T, on the average neutral loss rate, β_L (referenced to r_1), on the density of interstellar neutrals in the interstellar medium, n_∞, on the speed of the interstellar neutrals, v_0, and on the ratio of the force exerted by radiation pressure to the gravitational force, μ_0. In Table 1, we list the values of these parameters used for the calculations in this paper (for detailed discussions of these parameters, see *Geiss and Witte* [1996, and references therein]). We also list the production rates $\beta_p(r_1)$ used in our calculations.

Figure 3 shows diamonds that represent the observed distribution of hydrogen. For ion velocities, $0.8 < v'/u < 1.3$, SWICS samples the hydrogen population from the solar wind. For ion velocities outside this range, SWICS samples interstellar pickup hydrogen. Shown as the solid (dashed) curve is the numerically modeled spectrum given a 2 AU (0.01 AU) mean free path. The agreement between the observed and the modeled distribution is quite good.

The reader may note that the spectrum does not sharply cut off at $v' = 2u$. This gradual cutoff is caused by two effects: first, the ions are scattered in the wave frame with velocity $u\hat{\mathbf{e}}_r + V_A\hat{\mathbf{e}}_B$ measured from the spacecraft reference, where the Alfvén speed is given by $V_A = 50$ km/s; second, the solar wind speed fluctuates, and therefore a distribution of wind speeds, centered on the mean speed, must be used in the calculation.

In Figure 4, we show the observed and modeled distributions of interstellar pickup helium. The solid (dashed) curve represents the numerically modeled spectrum for a 0.8 AU (0.01 AU) mean free path.

The reason that shorter mean free paths yield sharper spectral knees near $w = 2$ in the spacecraft reference frame is made clear in Figure 1. The longer the mean free path, the longer it takes to scatter ions into the forward hemisphere. If this scattering time is comparable to the timescale of adiabatic cooling, ions will be strongly cooled before they are scattered into the forward hemisphere. Hence, in the case of a long mean free path, ions are substantially cooled before they are scat-

Table 1. Production Rates and Parameters Used in the Hot Model for the Interstellar Neutral Density

Species	T, K	β_L, 10^{-7} s^{-1}	n_∞, cm^{-3}	$\beta_p(r_1)$, 10^{-7} s^{-1}	v_0, km/s	μ_0
Hydrogen	8000	5.5	0.08	$\sim$ 1.5	20	0.8
Helium	7000	0.6	0.0155	$\sim$ 0.42	26	0

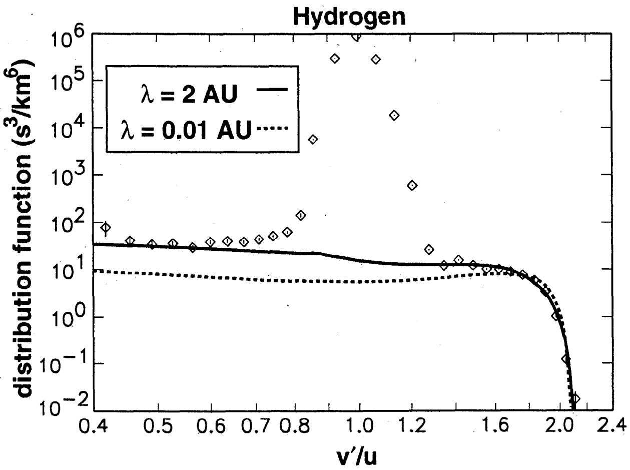

Figure 3. Comparison between the numerical model and data from Ulysses/SWICS (diamond symbols) for interstellar pickup hydrogen. The solid (dashed) curve was plotted for a 2 AU (0.01 AU) mean free path. Parameters of the model are described in section 5.

tered through 90° pitch angle which affects the shape of the spectrum.

6. Conclusions

Motivated by recent observations [*Gloeckler et al.*, 1995; *Fisk et al.*, 1997; *Möbius et al.*, 1997], we have described a transport model for pickup ions which assumes that ions are uniformly distributed in the forward and reverse hemispheres, with pitch angles $\theta < 90°$ and $\theta > 90°$, respectively. The transport equations may be solved using a simple, fast numerical algorithm.

In this paper, we examined two simple cases of pickup ion transport in which simple configurations were assumed for the plasma velocity and magnetic field structure. The transport equations, and the numerical algorithm can be generalized for more complicated configurations (*Schwadron et al.*, submitted manuscript, 1998). Comparisons were performed between the numerical solutions and previously derived analytical solutions. The model was also put to the test by performing detailed comparisons between modeled spectra and pickup ion spectra observed with the solar wind ion composition spectrometer on the Ulysses satellite: agreement between the modeled and observed distributions was quite good.

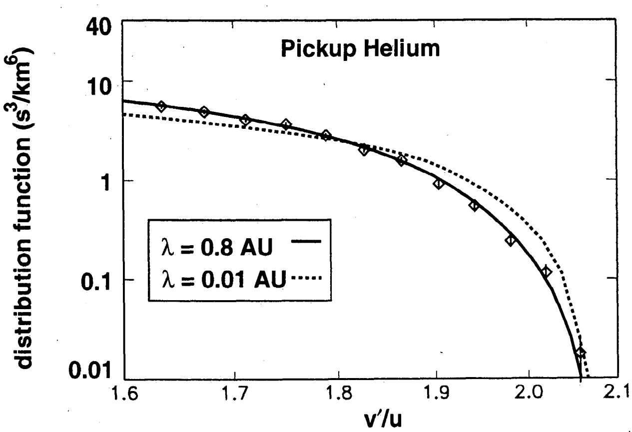

Figure 4. Comparison between the numerical model and data from Ulysses/SWICS (diamond symbols) for interstellar pickup helium. The solid (dashed) curve was plotted for a 0.8 AU (0.01 AU) mean free path. Parameters of the model are described in section 5.

Acknowledgments. The author gratefully acknowledges numerous stimulating discussions with Len Fisk, George Gloeckler, and Thomas Zurbuchen. This work was supported by NASA/JPL contract 955460, NASA grant NAG5-2810, and NASA grant NAS5-32626.

The Editor thanks Gary Zank and another referee for their assistance in evaluating this paper.

References

Bieber, J. W., W. H. Matthaeus, and C. W. Smith, Proton and electron mean free paths: the Palmer consensus revisited, *Astrophys. J.*, *420*, 294, 1994.

Bieber, J. W., W. Wanner, and W. H. Matthaeus, Dominant two-dimensional solar wind turbulence with implications for cosmic ray transport, *J. Geophys. Res.*, *101*, 2511, 1996.

Dusenbery, P. B., and J. V. Hollweg, Ion-cyclotron heating and acceleration of solar wind minor ions, *J. Geophys. Res.*, *86*, 153, 1981.

Fahr, H. J., The interplanetary hydrogen cone and its solar cycle variations, *Astron. and Astrophys.*, *14*, 263, 1971.

Fisk, L. A., N. A. Schwadron, and G. Gloeckler, Implications of fluctuations in the distribution functions of interstellar pick-up ions for the scattering of low rigidity particles, *Geophys. Res. Lett.*, *24*, 93, 1997.

Geiss, J., and M. Witte, Properties of the interstellar gas inside the heliosphere, *Space Sci. Rev.*, 78, 229, 1996.

Gloeckler, G., et al., The solar wind ion composition spectrometer, *Astron. Astrophys. Suppl. Ser. 92*, 267, 1992.

Gloeckler, G., N. A. Schwadron, L. A. Fisk, and J. Geiss, Weak pitch angle scattering of few MV rigidity ions from measurements of anisotropies in the distribution function of interstellar pickup H^+, *Geophys. Res. Lett.*, *22*, 2665, 1995.

Isenberg, P. A., A hemispherical model of anisotropic interstellar pickup ions, *J. Geophys. Res.*, *102*, 4719, 1997.

Matthaeus, W. H., M. L. Goldstein, and D. A. Roberts, Evidence for the presence of quasi-two-dimensional nearly incompressible fluctuations in the solar wind, *J. Geophys. Res.*, *95*, 20,673, 1990.

Möbius, E., D. Ruciński, M. A. Lee, P. A. Isenberg, Decreases in the anti-sunward flux on interstellar pickup He^+ associated with radial IMF, *J. Geophys. Res.*, *103,*, 257, 1998.

Palmer, I. D., Transport coefficients of low-energy cosmic rays in interplanetary space, *Rev. Geophys.*, *20* 335, 1982.

Parker, E. N., Dynamics of the interplanetary gas and magnetic fields, *Astrophys. J.*, *128*, 664, 1958.

Rowlands, J., V. D. Shapiro, and V. I. Shevchenko, Quasilinear theory of plasma cyclotron instability, *Sov. Phys. JETP, Engl. Transl.*, *23*, 651, 1966.

Ruciński, D., A. C. Cummings, G. Gloeckler, A. J. Lazarus, E. Möbius, and M. Witte, Ionization processes in the heliosphere - Rates and methods of their determination, *Space Sci. Rev.*, *78*, 73, 1996.

Skilling, J., Cosmic rays in the galaxy: Convection or diffusion?, *Astrophys. J., 170,* 265, 1971.
Thomas, G. E. The interstellar wind and its influence on the interplanetary environment, *Ann. Rev. Earth Planet. Sci., 6,* 173, 1978.
Vasyliunas, V. M., and G. L. Siscoe, On the flux and energy spectrum of interstellar ions in the heliosphere, *J. Geophys. Res., 81,* 1247, 1976.
Wu, F. M., and D. L. Judge, Temperature and flow velocity of the interplanetary gases along solar radii, *Astrophys. J., 231*, 594, 1979.
Zank, G. P., W. H. Matthaeus, J. W. Bieber, and H. Moraal, The radial and latitudinal dependence of the cosmic ray diffusion tensor in the heliosphere, *J. Geophys. Res., 103*, 2085, 1998.

N. A. Schwadron, Department of Atmospheric, Oceanic and Space Sciences, University of Michigan, 2455 Hayward Street, Ann Arbor, MI 48109-2143. (e-mail: nathanas@umich.edu)

(Received January 13, 1998; revised April 21, 1998; accepted May 11, 1998.)